Available online at www.sciencedirect.com
SCIENCE DIRECT®
Analytical Biochemistry 334 (2004) 20–35
ANALYTICAL BIOCHEMISTRY
www.elsevier.com/locate/yabio

Profiling the morphological distribution of O-linked oligosaccharides

Jinhua Zhang[a], Yongming Xie[a], Jerry L. Hedrick[b], Carlito B. Lebrilla[a,*]

[a] *Department of Chemistry and School of Medicine: Biological Chemistry, University of California, Davis, CA 95616, USA*
[b] *Department of Animal Science, University of California, Davis, CA 95616, USA*

Received 3 March 2004
Available online 24 August 2004

Abstract

The morphological distribution of oligosaccharides is determined in the egg jelly surrounding *Xenopus laevis* eggs. This biological system is used to illustrate a method for readily identifying and quantifying oligosaccharides in specific tissues. The extracellular matrix surrounding *X. laevis* eggs consists of a vitelline envelope and a jelly coat. The jelly coat contains three morphologically distinct layers designated J1, J2, and J3 from the innermost to the outermost and is composed of 9–11 distinct glycoproteins. Each jelly layer is known to have specific functions in the fertilization of the egg. We developed a rapid method to separate and identify the oligosaccharides from *X. laevis* egg jelly layers. Identification was based on the retention times in high-performance liquid chromatography (porous graphitized carbon column), exact masses, and tandem mass spectrometry. Over 40 neutral and 30 sulfated oligosaccharides were observed in the three jelly layers. Neutral oligosaccharide structures from different jelly layers were both unique and overlapping, while sulfated oligosaccharides were detected only in layers J1 and J2. Neutral oligosaccharides unique to jelly layer J3 and the combined layers J1 + J2 had similar core structures and similar residues. However, differences between these two sets of unique oligosaccharides were also observed and were primarily due to the branching carbohydrate moieties rather than the core structures.

Keywords: *Xenopus laevis*; Egg jelly layers; O-linked oligosaccharides; Structure elucidation; MALDI-CID-FTMS

The extracellular matrix surrounding the egg of the South African toad, *Xenopus laevis*, consists of a vitelline envelope and a thick outer jelly coat. The jelly coat contains three morphologically distinct layers designated J1, J2, and J3 from the innermost to the outermost (Fig. 1). The egg jelly coat layers are deposited around the eggs in the order of J1, J2, and J3 as they traverse the oviduct. It has been established that in amphibians the fertilization process is dependent upon the presence of jelly coat materials [1]. The proposed biological roles of egg jelly coat may include protection of eggs against pathogens, induction of sperm–egg binding/recognition, initiation of sperm capacitation and/or acrosome reaction, prevention of species cross-fertilization, and blockage of polyspermy [2–11]. These functions appear to be associated with particular jelly coat layers and are not properties of the jelly coat as a whole. However, the precise role that the egg jelly plays in fertilization is not fully resolved. It was demonstrated by Hedrick and co-workers [4] that full removal of the jelly coat resulted in a dramatic loss of egg fertilizability, while partially dejellied eggs (J3 removed) had fertilization rates comparable to those of untreated jellied eggs. The egg jelly has been postulated to act as a species-specific barrier to heterogonous sperm [3]. Video microscopy demonstrated that most sperm (over 97%) entering the jelly do not get to the egg surface but are trapped within J3 or at the outer surface of J2, with only 1–2% of the sperms that enter J3 actually arriving at the vitelline envelope [12]. These observations suggest that jelly coat molecules in individual layers play important roles in regulating sperm mobility within the jelly. One of the demonstrated functions of J1 is to interact with cortical granule lectin, a lectin released by the egg upon fertil-

* Corresponding author. Fax: +1 530 752 8995.
E-mail address: cblebrilla@ucdavis.edu (C.B. Lebrilla).

0003-2697/$ - see front matter © 2004 Elsevier Inc. All rights reserved.
doi:10.1016/j.ab.2004.07.012

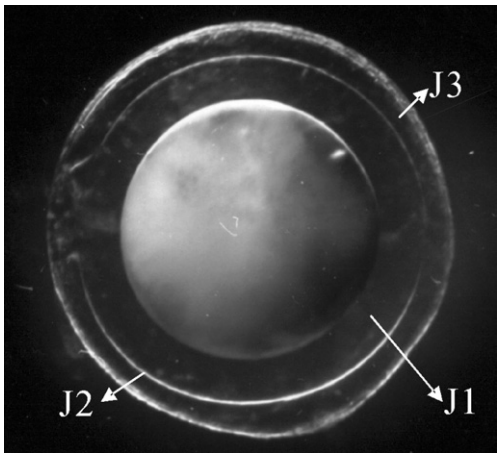

Fig. 1. The jelly coat consists of three distinct layers J1, J2, and J3 from the innermost to the outermost. These layers can be peeled manually under a microscope.

ization to form a fertilization layer that induces an irreversible change to the egg jelly coat, thereby establishing a block to polyspermy [13–15].

Analyses of the glycoproteins using gel electrophoretic, immunological, and ultracentrifugal methods have established that at least nine different glycoproteins are present in the three layers with J1, J2, and J3 having two or three, two, and four or five macromolecules, respectively. Each jelly coat layer is composed of 50–60% O-linked oligosaccharides [16]. Oligosaccharides are therefore key to many of the events leading to fertilization.

It has been postulated that oligosaccharides in the jelly coat may provide definite structural recognition sites [17]. The O-linked oligosaccharides in the jelly coat are highly heterogeneous in structure. In a previous study [18], we found nearly 30 neutral and over 47 anionic O-linked oligosaccharide components in the whole egg jelly glycoprotein. However, oligosaccharides in individual jelly layers have not been well characterized with respect to either their structure or their biological function. The elucidation of these oligosaccharide structures in specific jelly layers is an important step in the understanding of the relationship between structure and function of oligosaccharides, particularly of each layer during fertilization events.

Determination of oligosaccharide structures has always been a difficult task due to their large structure variation and complexity. In this study, we developed a rapid method that incorporates porous graphitized carbon solid-phase extraction (PGC-SPE)[1] cartridge, PGC-HPLC, matrix-assisted laser desorption/ionization Fourier transform mass spectrometry (MALDI-FTMS), and tandem mass spectrometry to separate and identify the oligosaccharides from the individual layers of *X. laevis* egg jelly coat.

Materials and methods

Mechanical dissection of X. laevis egg jelly layers

The mechanical dissection was performed under a dissecting microscope following the method published by Bonnell et al. [19,20]. The following procedure was used.

(1) Eggs were lifted away from De Boer's buffer solution (110 mM NaCl, 1.3 mM KCl, 1.3 mM $CaCl_2$, solid $NaHCO_3$ to yield pH 7.2) using watchmaker's forceps. The soft outermost layer J3 was then grasped firmly with a second pair of forceps and peeled away from the egg.
(2) Layer J2 is tougher and thinner. To remove J2, the egg was placed on a glass slide in a small volume of buffer (<100 μL) and pinned to the glass surface using two narrow-gauge syringe needles. A small incision was made in J2 by pulling the needles in opposite directions, keeping them against the glass surface. With J2 pinned to the surface by one needle, the J1-bound egg was pushed through the incision at its opposite end. J2 remained attached to J1 at the point where it was pinned to the glass slide and was cut away using a micro scalpel. J2 was invariably dissected with small amounts of adhering J1. Isolated J3 and J2 were dissolved in 0.3% (v/v) β-mercaptoethanol separately.
(3) J2-removed eggs were washed three times with Tris–De Boers buffer (110 mM NaCl, 1.3 mM KCl, 1.3 mM $CaCl_2$, 10 mM Tris–HCl, pH 8.9) and then solubilized with 0.3% (v/v) β-mercaptoethanol to extract the J1 layer.

To eliminate the oligosaccharide variability found between individuals, a single frog was used for this study. Two clutches of eggs were analyzed from the frog. The first clutch composed of 30 eggs was peeled to yield each egg jelly layer. A second clutch consisting of 50 eggs was peeled to yield the J3 layer. The J2 and J1 layers were left intact (J1 + J2) prior to release of the oligosaccharides.

Release and isolation of oligosaccharides

The solubilized jelly layers were dried in a Labconco RapidVac vacuum evaporation system. O-linked oligosaccharides were released from egg jelly glycoproteins by treating dried jelly layers with 1.0 M $NaBH_4$ and 0.1 M NaOH for 24 h at 42 °C. Then, 1.0 M hydrochlo-

[1] *Abbreviations used*: MALDI-CID-FTMS, matrix-assisted laser adsorption/ionization collision-induced dissociation Fourier transform mass spectrometry; Fuc, fucose; GlcNAc, *N*-acetylglucosamine; GalNAc, *N*-acetylglactosamine. PGC, porous graphitized carbon; SPE, solid-phase extraction; CLA, catalog-library approach; WGA; wheat germ agglutin.

ric acid solution was added to stop the reaction and destroy the excess $NaBH_4$ in an ice bath.

The resulting mixture of oligosaccharides was purified and fractionated on a (PGC-SPE) cartridge (Alltech Associates, Deerfield, IL). Prior to use, the PGC-SPE cartridge was washed with 80% (v/v) acetonitrile in 0.1% (v/v) trifluoroacetic acid followed by water. The sample was first loaded onto the SPE carbon column and allowed to run into the absorbents. Salts were washed off with water. Then, the column was treated with 10% and subsequently 20% (v/v) acetonitrile batch-wise to elute neutral oligosaccharides and finally with 40% (v/v) acetonitrile containing 0.05% trifluoroacetic acid to elute anionic oligosaccharides. For the J3 layer sample, all of the oligosaccharides eluted with only 40% (v/v) acetonitrile in 0.05% trifluoroacetic acid solution. The effluents from the PGC cartridge were collected in fractions with each fraction tested for the

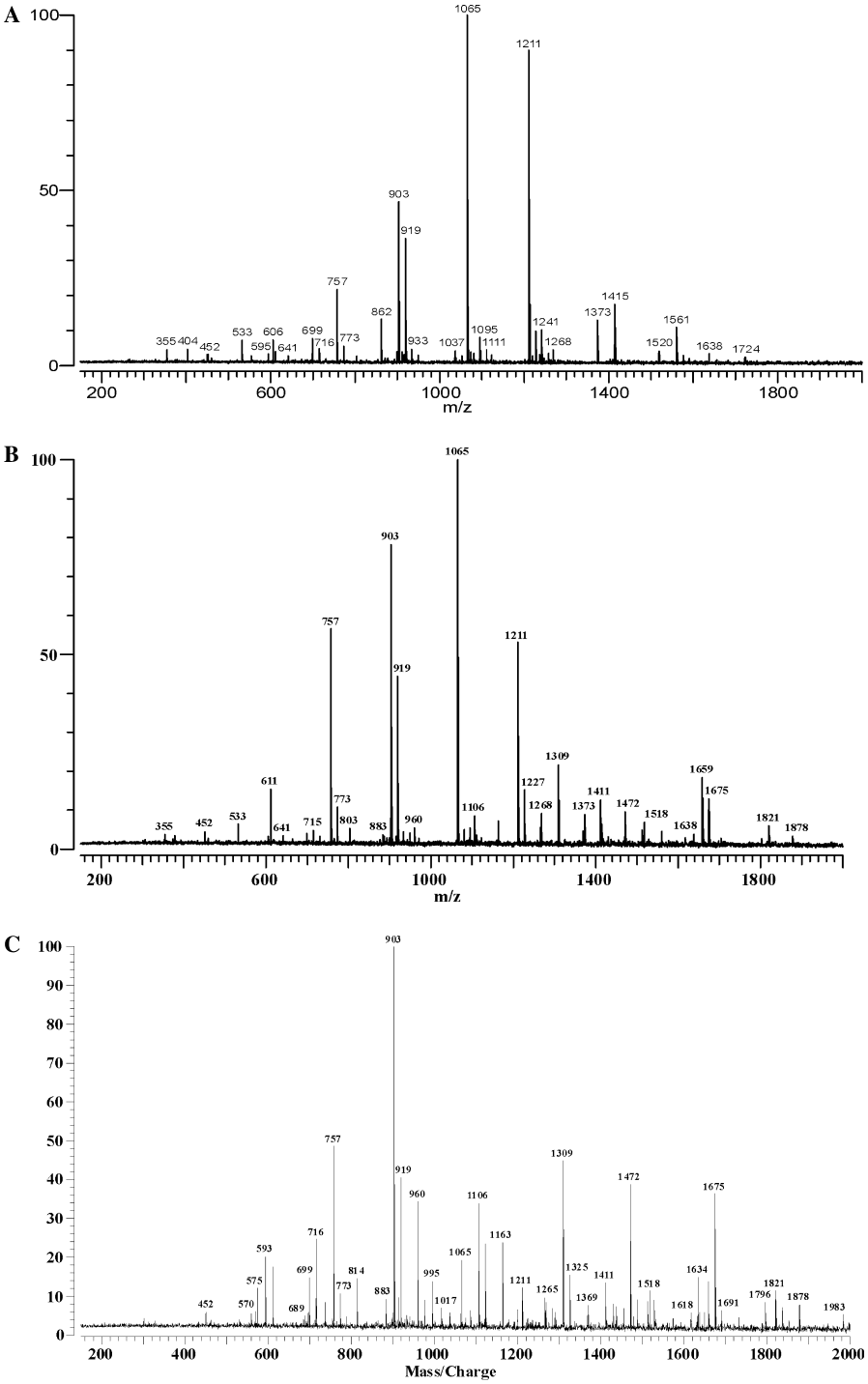

Fig. 2. MALDI-FTMS of neutral oligosaccharide components in individual jelly layers after PGC cartridge purification. (A) J3; (B) J2; and (C) J1.

oligosaccharide components by MALDI-FTMS. All fractions containing neutral and anionic oligosaccharides were combined, and the resulting samples were submitted for MS or HPLC.

HPLC separation

The glycan mixture from the PGC-SPE cartridge was injected into the HPLC equipped with a hypercarb porous graphitized carbon column (100 × 2.1 mm, 5 μm; ThermQ Hypersil Division, Bellfonte, PA). For the neutral oligosaccharides, a gradient of water and acetonitrile with a flow rate of 0.25 ml/min was used for the separation. The oligosaccharide alditols were detected at 206 nm. A total of 80 fractions were collected in 1-min intervals.

MALDI-FTMS analysis

A commercial MALDI-FTMS instrument (IonSpec, Irvine, CA), equipped with an external MALDI source, a 4.7-Tesla superconducting magnet, and a 337-nm

Table 1
Masses and compositions of neutral oligosaccharides in layers J3, J2, and J1

No.	Found	Expt. *m/z*	Theo. *m/z*	Hex	Fuc	HexNAc
1	J1, J3	449.172	449.174	0	0	2
2	J3	554.203	554.206	1	1	1
3	J1	570.196	570.201	2	0	1
4	J3	595.228	595.232	0	1	2
5	J1, J2, J3	611.223	611.227	1	0	2
6	J1, J3	716.253	716.258	2	1	1
7	J1, J2, J3	757.279	757.285	1	1	2
8	J1, J2, J3	773.273	773.280	2	0	2
9	J1	814.298	814.306	1	0	3
10	J3	862.307	862.316	2	2	1
11	J1, J2, J3	903.334	903.343	1	2	2
12	J1, J2, J3	919.329	919.338	2	1	2
13	J2, J1	960.354	960.364	1	1	3
14	J1	976.352	976.359	2	0	3
15	J1	1017.377	1017.386	1	0	4
16	J1, J2, J3	1065.384	1065.396	2	2	2
17	J1, J2	1106.410	1106.422	1	2	3
18	J1	1122.401	1122.417	2	1	3
19	J1, J2	1163.427	1163.444	1	1	4
20	J1, J2, J3	1211.438	1211.454	2	3	2
21	J2, J3	1227.431	1227.449	3	2	2
22	J1, J2, J3	1268.463	1268.475	2	2	3
23	J1, J2	1309.484	1309.502	1	2	4
24	J1	1325.476	1325.497	2	1	4
25	J2, J3	1373.489	1373.507	3	3	2
26	J2, J3	1414.512	1414.555	2	3	3
27	J1	1430.519	1430.528	3	2	3
28	J1	1455.532	1455.56	1	3	4
29	J1, J2	1471.530	1471.555	2	3	4
30	J1	1487.526	1487.55	3	1	4
31	J1, J2	1512.554	1512.581	1	2	5
32	J3	1519.525	1519.564	3	4	2
33	J1	1528.554	1528.576	2	1	5
34	J2, J3	1560.562	1560.591	2	4	3
35	J3	1576.556	1576.586	3	3	3
36	J1, J2	1617.600	1617.613	2	3	4
37	J1	1633.575	1633.607	3	2	4
38	J1	1649.552	1649.602	4	1	4
39	J1, J2	1658.604	1658.639	1	3	5
40	J1, J2	1674.603	1674.639	2	2	5
41	J1	1690.595	1690.629	3	1	5
42	J3	1722.597	1722.644	3	4	3
43	J1	1731.620	1731.656	2	1	6
44	J1	1795.616	1795.66	4	2	4
45	J1, J2	1820.646	1820.692	2	3	5
46	J1	1836.633	1836.687	3	2	5
47	J1, J2	1877.664	1877.713	2	2	6
48	J1	1982.706	1982.745	3	3	5

nitrogen laser, was used in this study as described in previous publications [18,21]. The MALDI sample was prepared by concentrating 1–20 μL of the HPLC fraction directly on the probe. For the positive mode, 1 μL of 0.1 M NaCl in ethanol/water solution (50:50 v/v) was added to the probe tip to enrich the Na^+ concentration and produce primarily sodiated species. One microliter of 0.4 M 2,5-dihydroxybenzoic acid in ethanol was added as the matrix. Warm air was used to quickly crystallize the sample on the probe. For the negative mode, 2.0 μL of saturated 2,5-dihydroxyacetophenone in ethanol was added on the probe tip as the matrix.

Collision-induced dissociation (CID)

A desired ion was readily selected in the analyzer with the use of an arbitrary wave form generator and a frequency synthesizer. All CID experiments were performed at 1000 Hz off resonance to the cyclotron frequency of the isolated ion. The CID excitation time was 1000–2000 ms. Two pulses of argon were introduced into the analyzer chamber at 0 and 500 ms for collision gas. The excitation voltages ranged from 3.0 to 8.0 V depending on the desired level of fragmentation and the size of the oligosaccharide.

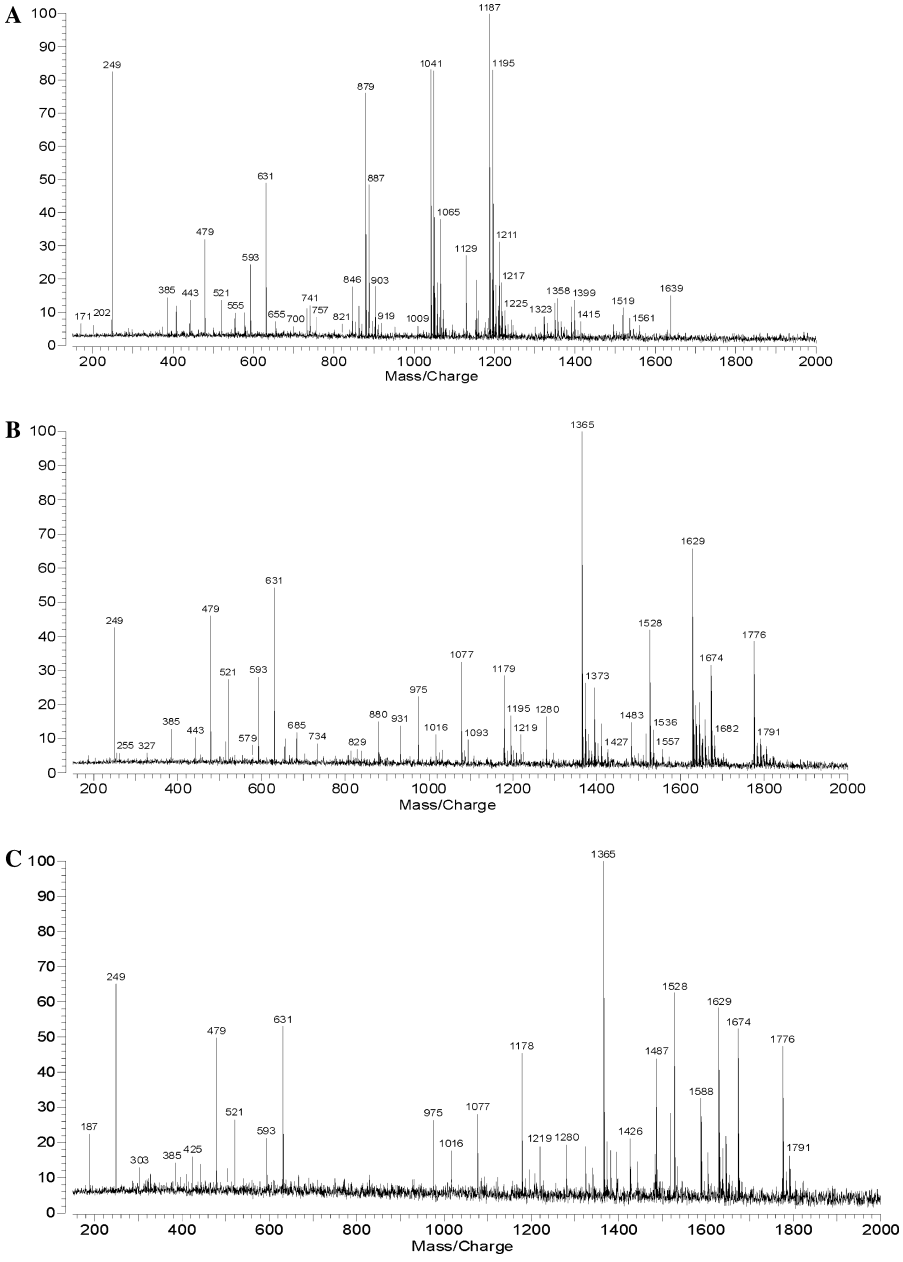

Fig. 3. MALDI-FTMS of anionic oligosaccharide components in individual jelly layers after PGC cartridge purification. (A) Mass spectrometry analysis of J3 glycans in the negative mode (most signals corresponded to deprotonated neutral oligosaccharides); (B) negative mode of J2 anionic components; and (C) negative mode of J1 anionic components.

In situations where CID would not produce all necessary fragments, "in-source dissociation" was used. This technique employed elevated MALDI laser power to produce fragment ions of pure compounds directly in the source. It was found that the ions produced were similar to those produced by CID, but more extensive fragmentations were observed.

Results

Mass spectrometric analysis of oligosaccharide mixtures in individual jelly layers

The high sensitivity of mass spectrometry was used to minimize the potentially laborious effort of physically removing the layers from hundreds of egg. For these experiments, a relatively small number of eggs, 30–50, were "peeled." After release of the oligosaccharides, the sample was passed over a PGC-SPE cartridge to isolate the neutral and anionic components from the salts and peptide components (see Materials and methods).

The collected PGC-SPE fractions were pooled to contain both neutral and anionic oligosaccharides, concentrated, and analyzed by MALDI-FTMS. Two groups of eggs from a single frog were collected to illustrate the differences in oligosaccharide compositions in the three layers. In the first pool each layer was individually peeled and analyzed. The outermost layer (J3) was the thickest (200 μm) and the easiest to remove. The isolated neutral components were analyzed by MALDI-FTMS

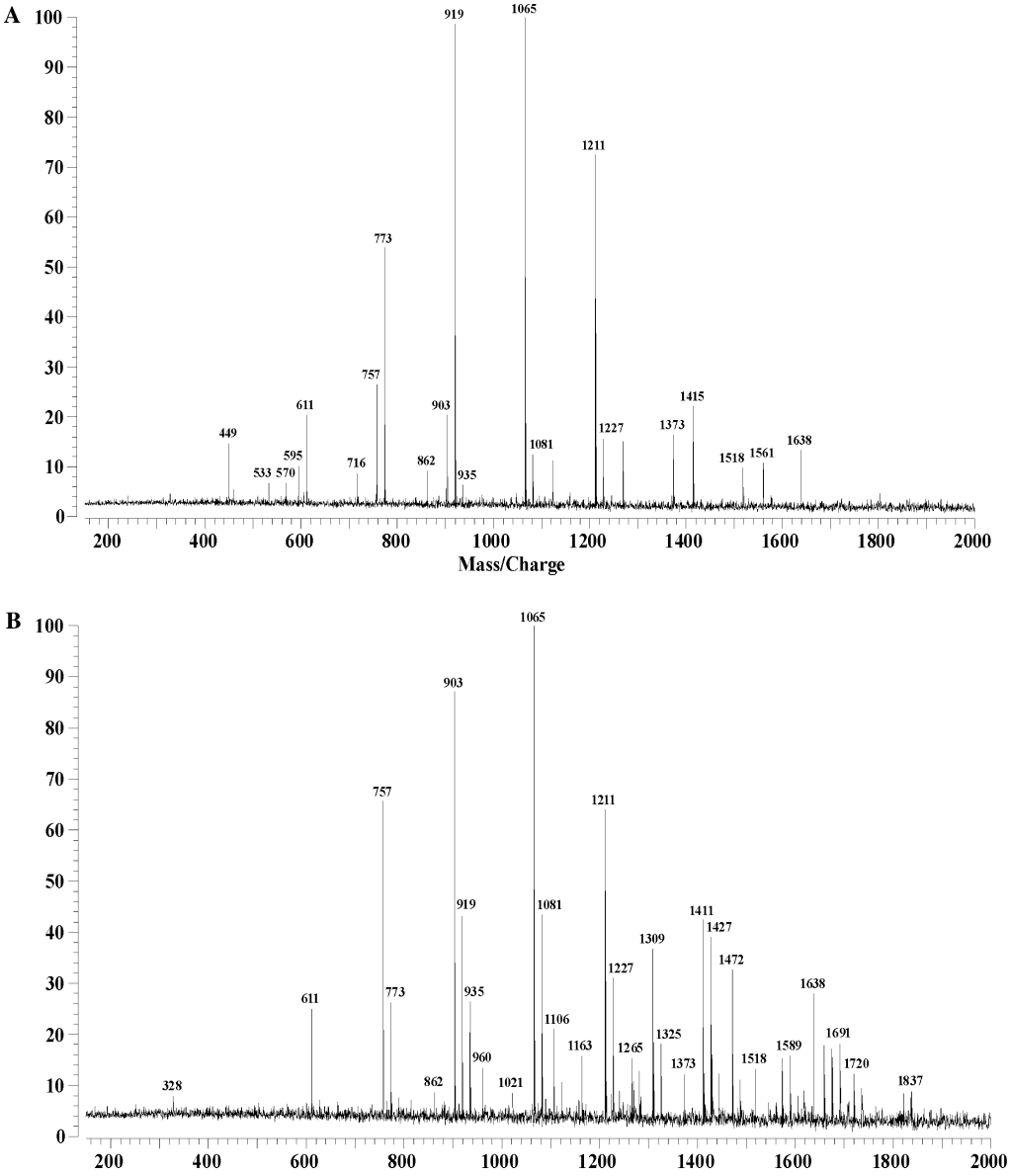

Fig. 4. MALDI-FTMS of neutral and anionic oligosaccharide mixtures in layers J3 and J1 + J2 after PGC cartridge purification. (A) Positive mode of J3 neutral components; (B) positive mode of J1 + J2 neutral components; (C) negative mode of J3 glycans (most signals corresponded to deprotonated neutral oligosaccharides); and (D) negative mode of J1 + J2 anionic components.

and the resulting spectrum is shown in Fig. 2A. Nearly all the observable peaks corresponded to neutral oligosaccharides as determined by accurate mass analyses.

The second layer (J2) is the thinnest (15 μm) and yielded the positive ion spectra shown in Fig. 2B. It was extremely difficult to totally remove J2 from the innermost and relatively thicker layer J1 (150 μm) without cross contaminating the layers. The thinness of J2 and the swelling of J1 upon removal of J2 made it difficult to remove J2 with the complete exclusion of parts of J1. For these reasons, we believed that J2 samples contained some amounts of J1. In any case, the J2 sample presented here was our best attempt at separating the two layers. The spectrum shown in Fig. 2B shows the oligosaccharide distribution in J2 centered at a lower mass than that found in J3. The neutral components of J1 were examined and the positive ion spectrum of the mixture is shown in Fig. 2C. The neutral components appeared to be distributed over a broader mass range with enhanced representation of larger oligosaccharides. Note that the mass spectra of the J2 layer appear to be a combination of the J1 and J3 layers.

In addition to the general differences between the appearances of the three spectra, there were specific peaks that were found in two or only one of the spectra. For example, *m*/*z* 1309 was an abundant peak found in J2 and J1 but not in J3. Conversely, *m*/*z* 862 was found primarily in J3. There were similarly differences in the relative abundances of several peaks. For example, *m*/*z* 1065 and *m*/*z* 903 were abundant in all three layers, however, the ratios of the two peaks were significantly different in the three layers, being (I_{903}/I_{1065}) 0.47 in layer J3, 0.78 in layer J2, and 5.2 in J1. The summary of the masses corresponding to neutral oligosaccharides at each layer is tabulated in Table 1.

For J1 and J2, the anionic and neutral components were eluted separately by the proper selection of the eluting solvents. For J3, all oligosaccharides were eluted under a single elution (see Materials and methods). The negative ion mass spectra of the mixtures from individual

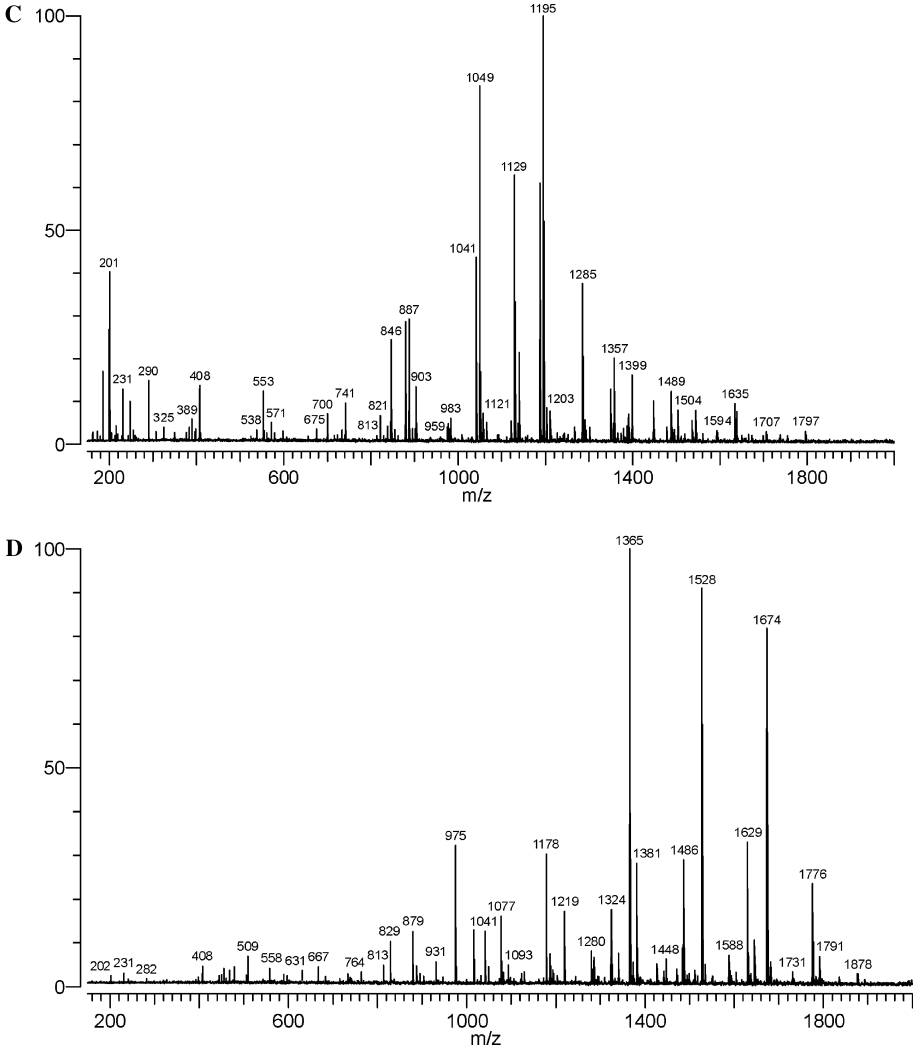

Fig. 4. (*continued*)

layers are presented in Fig. 3. All anionic oligosaccharides in the negative mode were observed in the -1 charge state. The signals observed from the J3 layer were primarily deprotonated neutrals. The analyses of each peak based on the exact mass did not yield a single sulfated species. Based on the mass spectra of the individual layers, we concluded that sulfated oligosaccharides were present only in J2 and J1. It is necessary to point out that sulfated ($R\text{-}SO_4^-$) and phosphated ($R\text{-}HPO_4^-$) species have similar masses differing only by 0.0095 amu, which is difficult to differentiate even with the high mass resolution of the FTMS. However, with $R\text{-}HPO_4^-$, we would also expect to observe $R\text{-}NaPO_4^-$ because H^+ is often replaced by Na^+ in the MALDI-MS analyses of carboxylic acid-, sulfate-, and phosphate-attached oligosaccharides. There were no signals corresponding to $R\text{-}NaPO_4^-$ in any of the negative-mode spectra, therefore we assumed that we observed only $R\text{-}SO_4^-$ species. Furthermore, there have been no reports of phosphated oligosaccharides in the amphibian egg jelly.

Because of the distinct differences between the J3 and the J1 and J2 layers and the difficulty in obtaining pure J2, it was decided that J3 would be examined separately while J1 and J2 would be combined to confirm that there were no sulfated oligosaccharides in J3 and that there were neutrals in the J1 + J2 layers. An additional group of 50 eggs was peeled and examined as before with the J3 removed and the J1 + J2 left intact prior to the release of the oligosaccharides. The analyses of these two samples in both the positive and the negative modes confirmed that the sulfated oligosaccharides were present only in the J1 + J2 sample (Fig. 4). A total of 22 O-linked singly sulfated and 9 doubly sulfated oligosaccharide components (Table 2) were detected in inner J1 + J2 layers.

Identification and structural elucidation of neutral oligosaccharide components

The majority of the oligosaccharide structures in the egg jelly have been previously elucidated [18]. To determine the identity of the oligosaccharides, a combination of retention time, exact mass, and CID was used to compare known samples from previous studies with those found in this one. Each oligosaccharide component has a unique structure that yields a distinct fragmentation pattern. To determine the structures of new compounds, we employed further CID to identify specific structural motifs (catalog-library approach; CLA [21]).

Table 2
Masses and compositions of anionic oligosaccharides (found only in layers J1and J2)

No.	Expt. *m/z*	Theo. *m/z*	Hex	Fuc	HexNAc	Na	Sulfate
1	407.168	407.086	1	1	0		1
2	505.135	505.134	0	0	2		1
3	667.191	667.187	1	0	2		1
4	813.247	813.245	1	1	2		1
5	829.242	829.240	2	0	2		1
6	931.183	931.179	2	0	2	1	2
7	975.301	975.298	2	1	2		1
8	1016.328	1016.324	1	1	3		1
9	1032.323	1032.319	2	0	3		1
10	1073.354	1073.346	1	0	4		1
11	1077.240	1077.236	2	1	2	1	2
12	1178.382	1178.377	2	1	3		1
13	1203.452	1203.409	0	2	4		1
14	1219.407	1219.404	1	1	4		1
15	1280.320	1280.316	2	1	3	1	2
16	1324.441	1324.435	2	2	3		1
17	1340.433	1340.430	3	1	3		1
18	1365.466	1365.462	1	2	4		1
19	1381.460	1381.456	2	1	4		1
20	1483.400	1483.395	2	1	4	1	2
21	1486.495	1486.513	3	2	3		1
22	1527.517	1527.514	2	2	4		1
23	1588.428	1588.427	3	2	3	1	2
24	1629.453	1629.453	2	2	4	1	2
25	1645.430	1645.448	3	1	4	1	2
26	1673.576	1673.573	2	3	4		1
27	1730.602	1730.594	2	2	5		1
28	1775.513	1775.512	2	3	4	1	2
29	1791.485	1791.485	3	2	4	1	2
30	1835.623	1835.626	3	3	4		1
31	1876.657	1876.652	3	3	5		1

The PGC column provided a high-resolving HPLC separation of O-linked oligosaccharide mixtures. This method has been used extensively to separate a wide range of glycans [22–24]. Fig. 5 shows the HPLC chromatograms of neutral oligosaccharides in the J3 layer and the combined J1 + J2 layers. These two experiments were carried out under identical conditions. Under our HPLC conditions neutral oligosaccharide components elute between 3 and 45 min. Based on the relative abundances of the components in the HPLC trace, we concluded that the J3 layer had the largest abundances of neutral components. The combined J1 and J2 layers (J1 + J2) had fewer neutral components but appeared to have a greater variety of individual components.

The majority of the HPLC peaks contained a single component. Individual collected fractions, however, contained more than one peak as the collection was performed in 1-min increments and could not be timed with the elution of specific peaks. However, isomers had sufficiently different retention times and were rarely contained in a single fraction. For example, there were four isomers for *m*/*z* 1065. In the J3 layer these compounds were found at 14.98, 38.72, and 43.50 min. In the J1 + J2 sample, they were found at 14.98, 40.10, and 43.17 min. The J3 layer contained one isomer that was not found in the J1 + J2 layer (38.72 min), while the isomer at 40.10 min was found only in the J1 + J2 sample. There was more retention time variation found in the sample that eluted at 43 min as the peak was broader and contained an additional component in the J1 + J2 sample. Nonetheless, the retention time was sufficient to allow complete isolation of the different isomers from each other.

To confirm the identity of these compounds, we employed the method of CLA to verify structures [21]. In this method collision-induced dissociation is used to determine the presence of structural motifs based on the fragmentation patterns. A catalog of five motifs

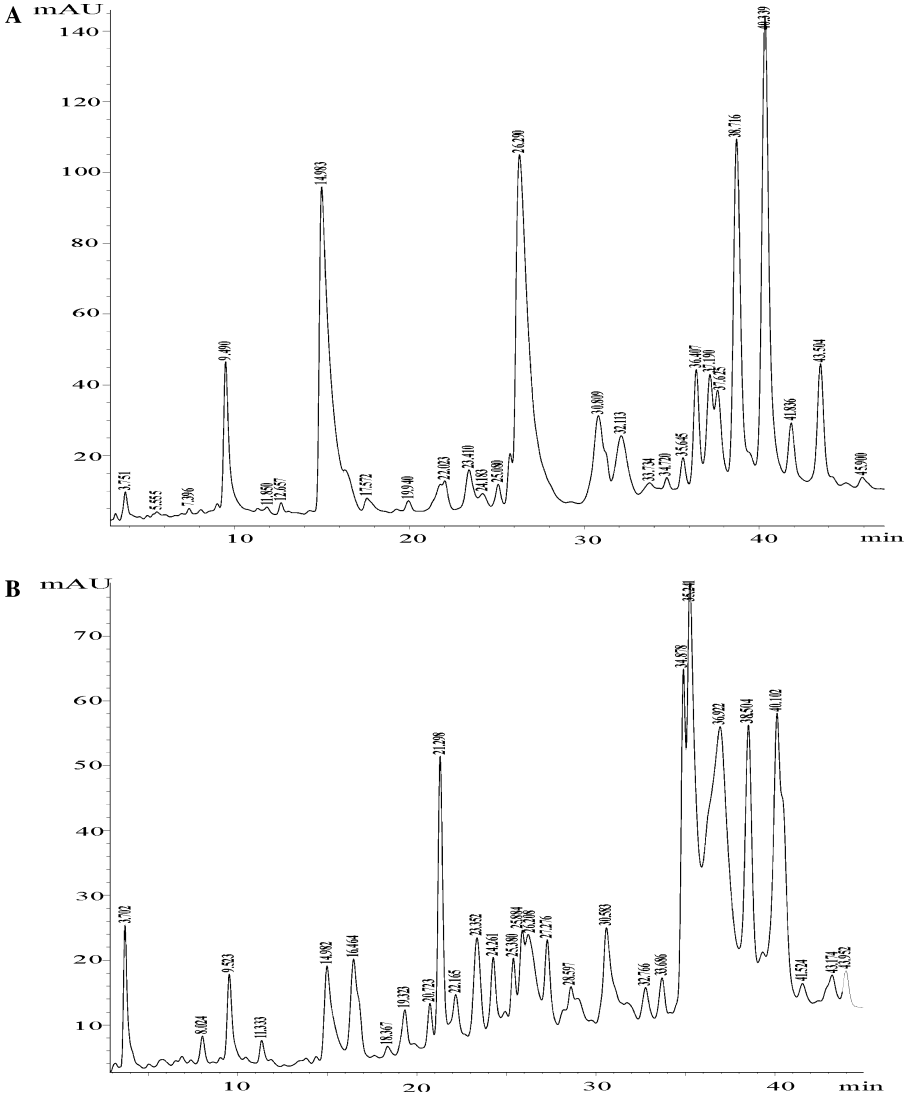

Fig. 5. HPLC chromatograms of the neutral oligosaccharide mixture from layers J3 (A) and J1 + J2 (B).

was constructed from tandem MS studies of 12 oligosaccharides whose structures were initially determined by NMR [25]. Based on the CID spectra of the compound, specific structural motifs were found and pieced together to provide the complete structure. The method was described extensively in earlier publications [21]. It was further validated by the use of exoglycosidase digestion to confirm the structures obtained by CLA [26]. This method has been used to determine the structures of more than 20 unknown neutral oligosaccharides in the egg jelly of *X. laevis* [18].

To illustrate the features of CLA, the four *m/z* 1065 isomers were identified. The composition was predicted from the exact mass to be 2 Hex, 2 Fuc, and 2 HexNAc. The tandem MS spectra of the compound in fraction 15 from both J1 + J2 and J3 samples are shown in Fig. 6.

The structures based on these motifs are presented (Fig. 6B, inset). Motif **iii** was characterized by the presence of the *m/z* 347 which is characteristic of the Gal(β1-3)Gal(β1-3) fragment coordinated to Na^+. It is also characterized by the loss of fucose in the presence of a weak loss of Hex from the quasimolecular ion $[M + Na]^+$. The MS^4 spectrum yields the presence of motif **i**. This motif is characterized by the presence of several peaks including *m/z* 611, 449, 408, 431, and 413. The structure is consistent with the previously determined compound **XL-1065-1**. All four compounds have the same core as evidenced by the presence of these ions in the MS^4 spectra.

Variations between the other isomers are found in the nonreducing end. Fraction 38 from both samples contains an isomer whose tandem MS spectrum is shown in Fig. 7. This compound similarly contains motif **iii** due to the presence of the fragments described above. It differs from the previous compound by the position of a Fuc, which is now on the GlcNAc rather than the terminal Gal. The loss of Hex, though small, is reproducible. The presence of this ion and the absence of the loss of HexNAc indicate that the Fuc is on the GlcNAc residue. This compound is a new structure that has not been determined previously and is numbered **XL-1065-4.**

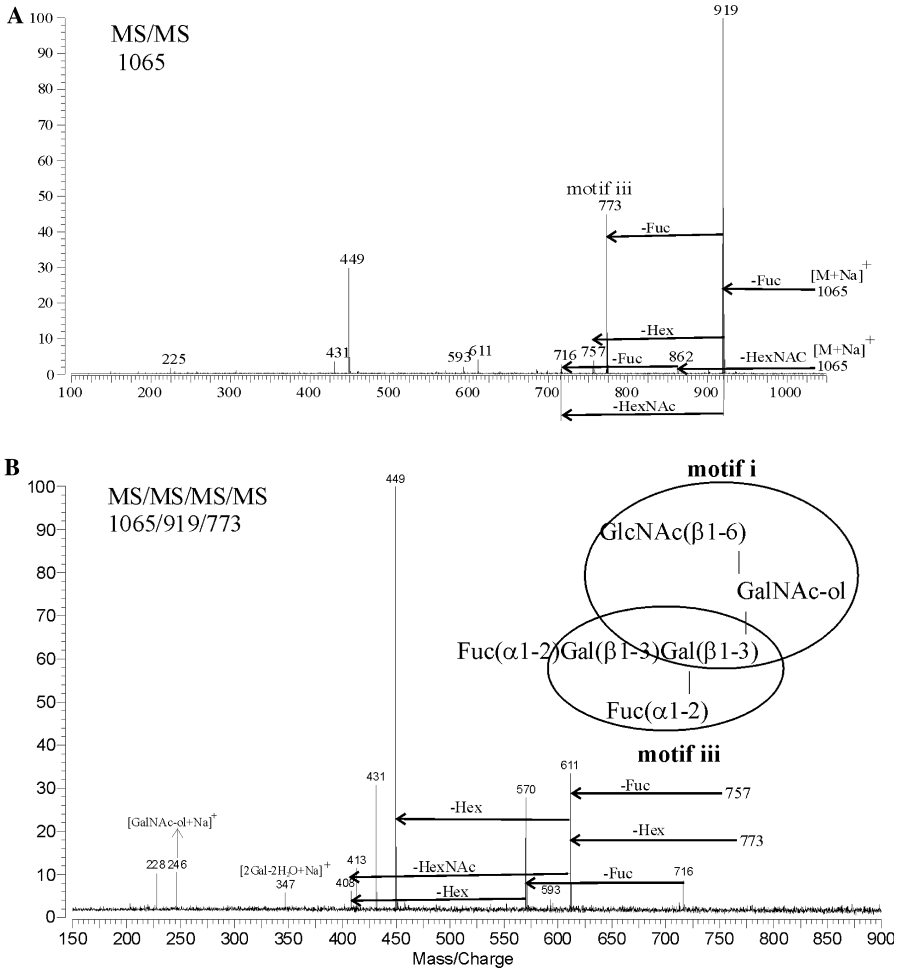

Fig. 6. CID spectra of **XL-1065-1** in fraction 15 from layers J3 and J1 + J2. (A) MS/MS spectrum; (B) MS/MS/MS/MS spectrum (*m/z* 1065 →*m/z* 919 → *m/z* 773).

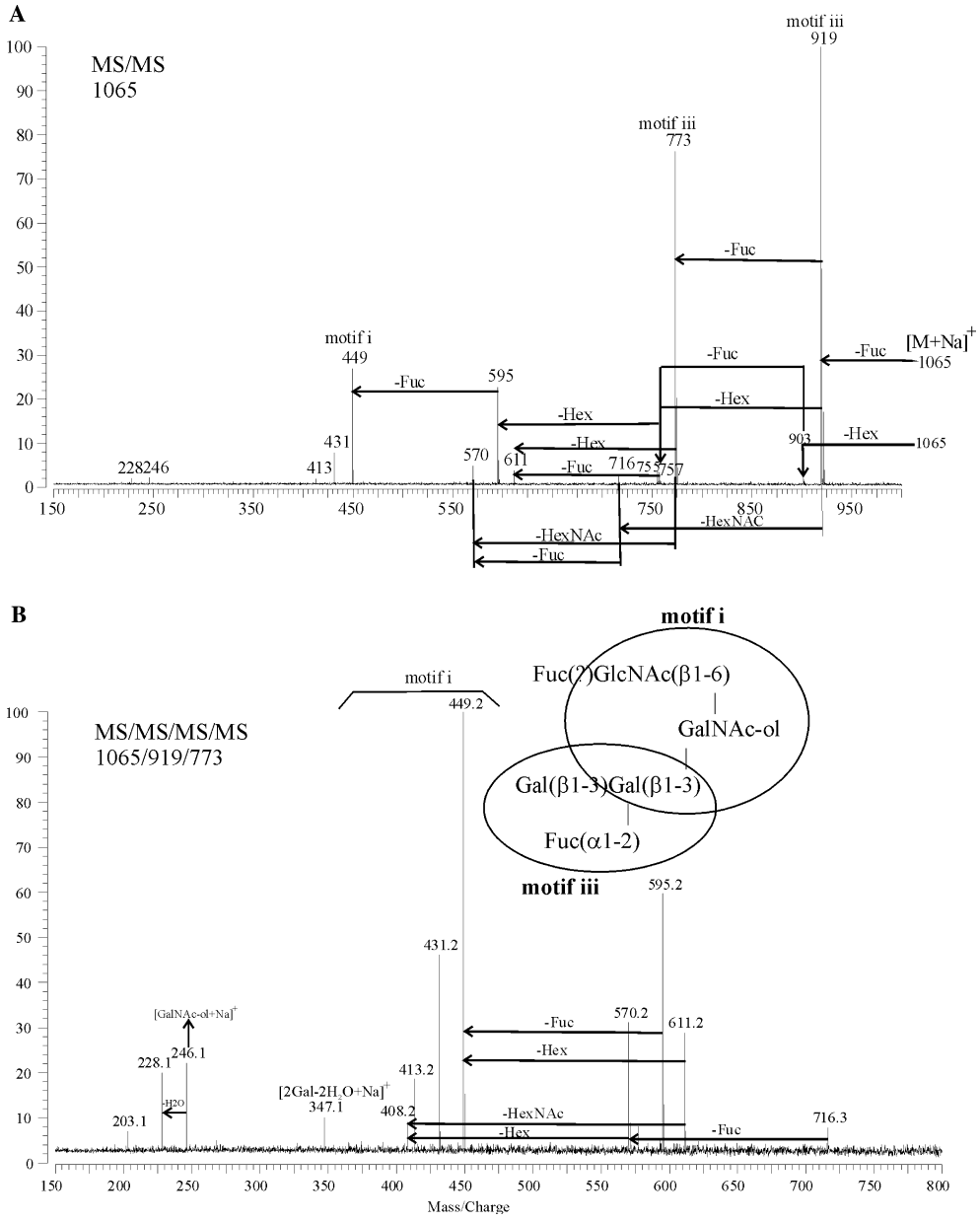

Fig. 7. CID spectra of **XL-1065-4** in fraction 38 from layer J3. (A) MS/MS spectrum; (B) MS/MS/MS/MS spectrum (*m*/*z* 1065 → *m*/*z* 919 → *m*/*z* 773).

The compound in fraction 43 contains a different motif that is characterized by the relatively abundant loss of the Hex and Fuc from the quasimolecular ion. This fragmentation pattern has been earlier assigned to motif **ii** (Fig. 8, inset). This novel compound is numbered **XL-1065-5**.

The fourth isomer from fraction 40 (in Fig. 9) contains a common core, however, it also contains a hexose residue bonded to the GlcNAc branch. The presence of *m*/*z* 388.1, a Hex-HexNAc fragment coordinated to Na^+ verifies the structure. The structure matches a previously known compound (**XL-1065-3**). Because all the hexoses have been exclusively Gal in oligosaccharides from egg jelly of *X. laevis* [25,27], the hexose present in all structures is assigned accordingly. The confirmation of this structure by exoglycosidase reaction has been performed.

Totals of 17 and 20 neutral oligosaccharide structures were determined in layers J3 and J1 + J2, respectively. The complete list of neutral oligosaccharides common to layers J3 and J1 + J2 are presented in Chart 1. The fraction numbers signify the collection times (in minutes) and are directly correlated to Fig. 5. A few of the structures belonging to minor components could not be determined completely as there were limited amounts for the full CLA treatment. Nonetheless, the sequences

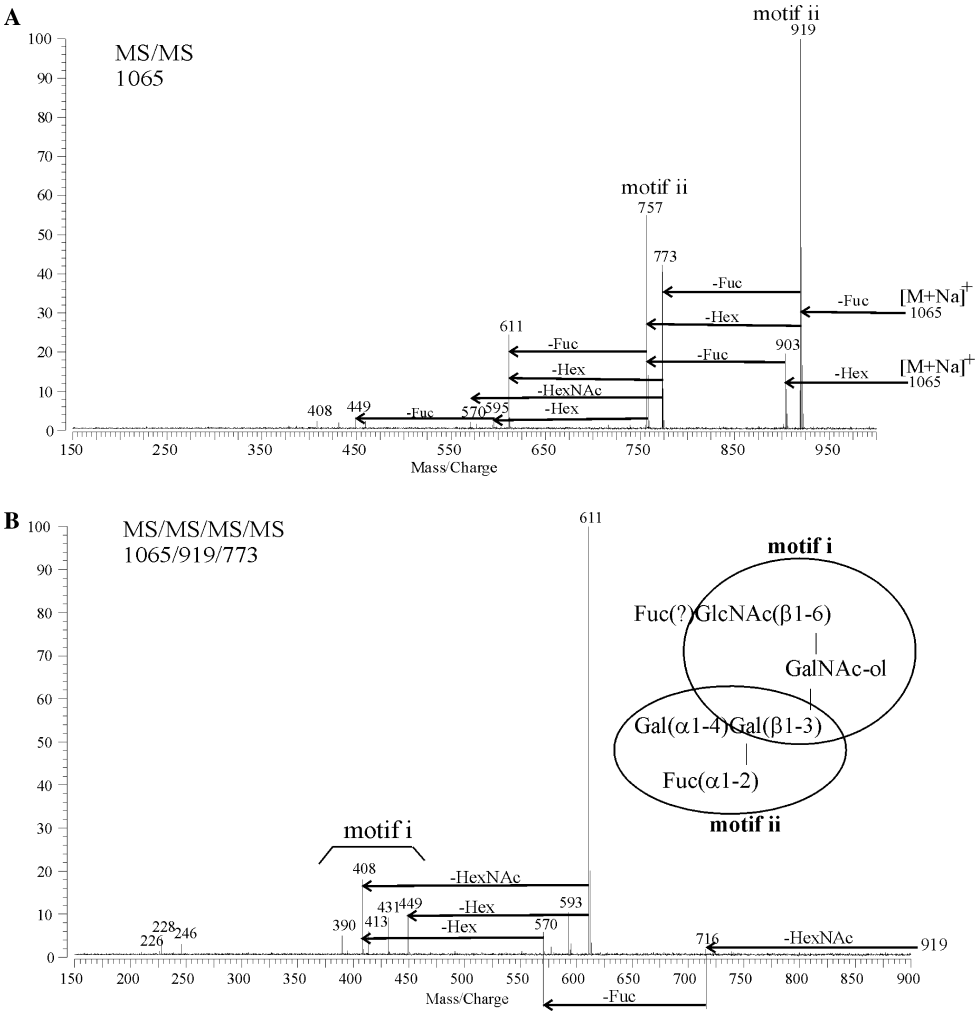

Fig. 8. CID spectra of **XL-1065-5** in fraction 43 from layers J3 and J1 + J2. (A) MS/MS spectrum; (B) MS/MS/MS/MS spectrum (*m/z* 1065 → *m/z* 919 → *m/z* 773).

of the oligosaccharides were determined by CID and are provided.

All the anionic (sulfated) oligosaccharides were found only in the J1 + J2 sample. The neutral oligosaccharides were found in all three layers. Their distributions between J3 and J1 + J2 are provided in Charts 1, 2, and 3. Ten oligosaccharides were common to both J3 and J1 + J2 (Chart 1). Most of these oligosaccharides had essentially the same trisaccharide core structure. Branching occured through both the GlcNAc and the Gal residues. Some structures, however, were unique to a specific source. Neutral oligosaccharides unique to either J3 or J1 + J2 have the same set of core structures. All are similarly focusylated structures. The differences were primarily due to the branching moieties rather than the core structures. For oligosaccharides unique to layer J3, single or multiple Gal residues are attached to the Gal(β-) branch of the core structure. Oligosaccharides unique to J1 + J2 contain single or multiple HexNAc residues that are typically attached to the Gal(β-) branch of the core structure.

Quantitation of oligosaccharide components

The quality of the separation of the oligosaccharides in the PGC column and the sensitivity of the detection with the diode array detector allowed quantitation of the individual components. The chromophore at 206 nm is the *N*-acetyl group in the hexosamine residues. To determine the detector response a small study with commercially available model compounds was conducted. Five compounds were examined, including maltohexaose, lacto-*N*-fucopentose II, lacto-*N*-hexaose, *N*,*N*′,*N*″-acetyl-chitotriose, and tetra-*N*-acetyl-chitotetraose, with a varying number of *N*-acetylhexoseamine residues from 0 to 4, respectively. The detector response for 10 nmol was measured for each compound with the results presented in Table 3. When an *N*-acetylhexoseamine residue is absent, there is no detectable response on the detector. However, the response does not scale linearly with the number of *N*-acetylhexoseamine residues. There are a number of reasons for this behavior, mainly structural; however, it is clear that the

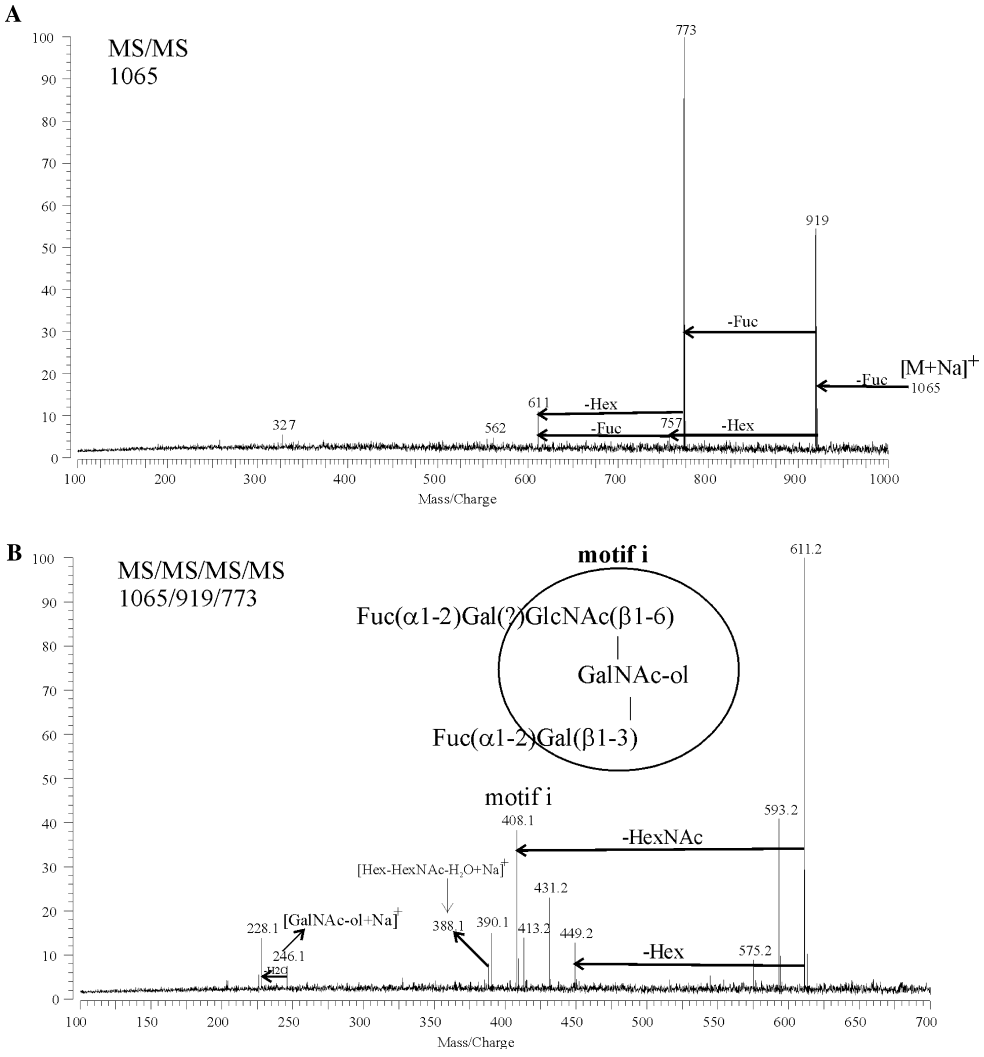

Fig. 9. CID spectra of **XL-1065-3** peak in fraction 40 from layer J1 + J2. (A) MS/MS spectrum; (B) MS/MS/MS/MS spectrum (*m/z* 1065 → *m/z* 919 → *m/z* 773).

presence of the residue allows the compounds to be readily observed.

Employing the relative response from the standard compounds, the quantity of each component was assigned in Charts 1, 2, and 3. The value listed is relative to that of the most abundant component. For example, in the J3 layer **XL-1211-1** is the most abundant component while it is of moderate abundance in the J1 + J2 layer. The most abundant species in J1 + J2 is **XL-1065-1**, which is of moderate abundance in the J3 layer.

Discussion

The majority of the neutral oligosaccharides are present in the J3 layer. The combined J1 + J2 layers have approximately half the amount of neutral carbohydrates but all the sulfated species. In the neutral oligosaccharides of J3, there are four components that make up nearly 80% of the total. Despite the large number of different structures, the four most abundant oligosaccharides (**XL-1065-1, XL-1211-1, XL-903-2,** and **XL-1065-4**) share a common structural feature. The central core is the same and elongation occurs primarily through the Gal(β) branch by Gal(β1-3) to yield a Gal(β1-3)Gal(β1-3) motif. Structural diversity is obtained from varying degrees of fucosylation. This motif represents the ubiquitous sequence in glycan structures of amphibian egg jelly [27].

The distribution of the oligosaccharides in the layers appears consistent with a number of observations reported in the literature with regard to the biological role of the egg jelly. The sulfated oligosaccharides are primarily found in the innermost J1 layer. There were sulfated oligosaccharides present in the J2 layer sample, however it was difficult to determine whether these originated within the layer or were a contamination from J1.

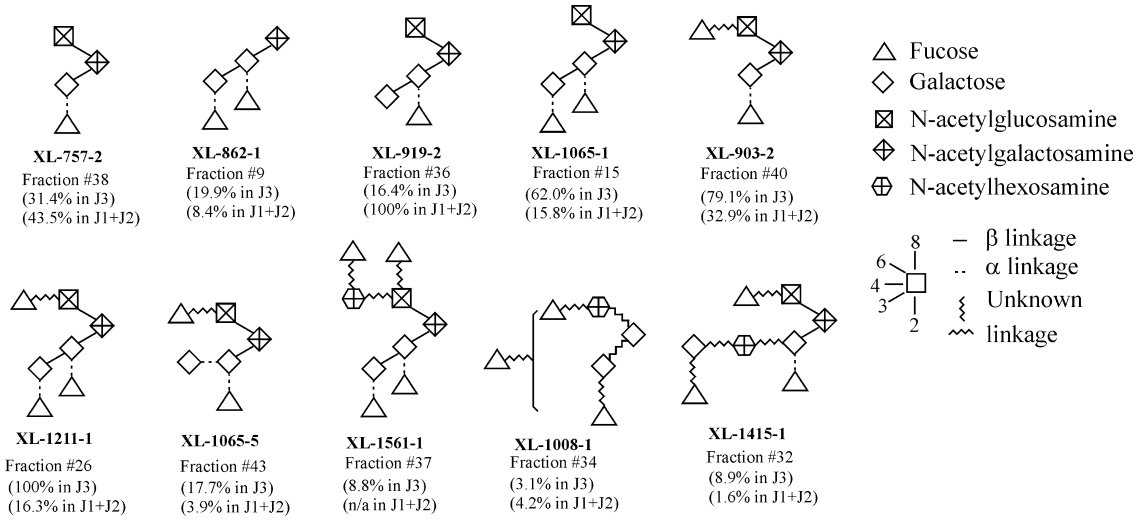

Chart 1. Oligosaccharide structures common to all three layers. The relative abundance of each component in parentheses is based on the peak area ratio relative to the most abundant compound in the layer.

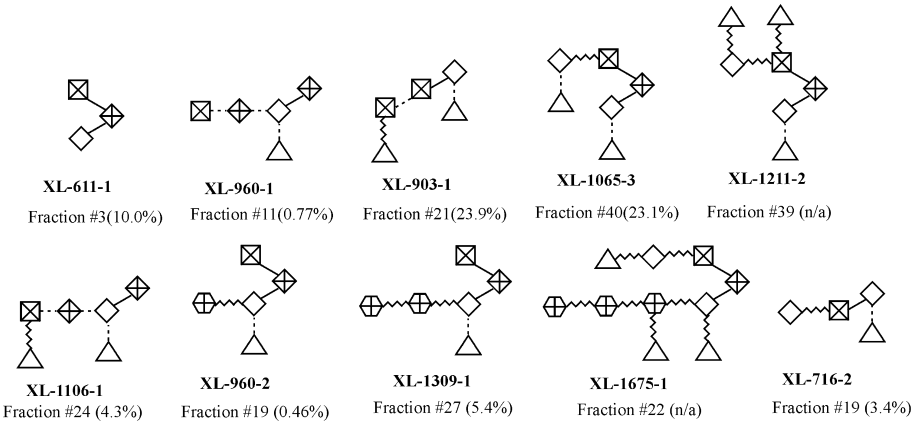

Chart 2. Oligosaccharide structures unique to layer J1 + J2. The relative abundance of each component in parentheses is based on the peak area ratio relative to the most abundant compound in the layer. For J1 + J2, the most abundant compound is **XL-919-2**.

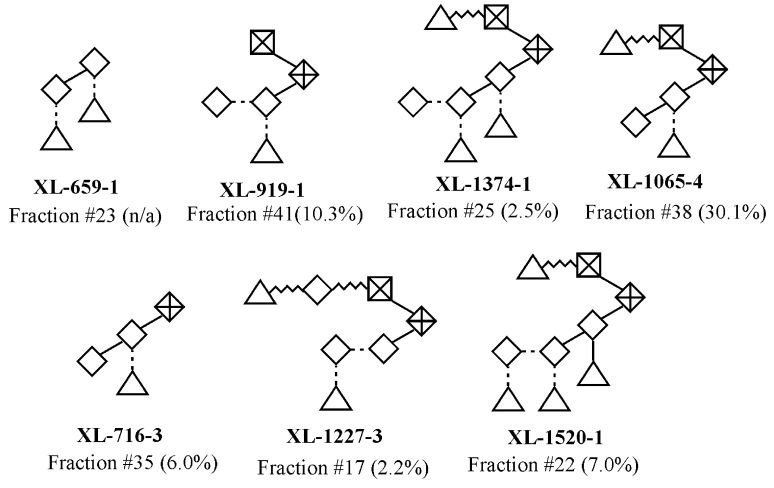

Chart 3. Oligosaccharide structures unique to layer J3. The relative abundance of each component in parentheses is based on the peak area ratio relative to the most abundant compound in the layer. For J3, the most abundant compound is **XL-1211-1**.

Table 3
UV absorption response (at 206 nm) of five standard oligosaccharides with different numbers of *N*-acetyl groups (10 nmol amount)

Oligosaccharide (10 nmol)	Number of *N*-acetyl groups	Corresponding HPLC peak area (mAU*s)	Response ratio relative to chitotriose
Maltohexaose	0	0	0
Lacto-*N*-fucopentose II	1	8659	0.46
Lacto-*N*-hexaose	2	9760	0.52
N,*N*′,*N*″-acetyl-chitotriose	3	18947	1.00
Tetra-*N*-acetyl-chitotetraose	4	16782	0.89

Hedrick and co-workers [16] have reported, based on the chemical analysis of the individual layers, that the majority of the sulfate was found in the J1 layer . Furthermore, ^{35}S injected into the frog was found incorporated into the J1 layer [28]. Cellulose acetate electrophoresis of J1 yielded two anodically migrating components [16]. While these studies suggested that the sulfates were in the J1 layer presumably in the form of carbohydrates, the results presented here provide the first confirmation that the sulfates are indeed in the carbohydrate forms.

The *N*-acetylglucosamine distribution is important as wheat germ agglutin (WGA), a lectin specific for the binding of *N*-acetylglucosamine, is known to inhibit sperm penetration. Exposure of the egg jelly to WGA slightly diminishes sperm penetration in the J3 layer and blocks completely the progression through the inner J2 and J1 layers. *N*-acetylglucosamine is found in every layer. The structures that are common to all three layers contain a number of oligosaccharides that have *N*-acetylglucosamine, many in the nonreducing end. However, oligosaccharides unique to the J1 and J2 layers contain this monosaccharide residue while those unique to J3 do not generally contain this residue on the nonreducing end.

Conclusion

From the distribution of oligosaccharides and some known functions of the layers, we may make some general hypotheses with regard to the relationship between function and structure in oligosaccharides. The outermost J3 layer is composed primarily of neutral oligosaccharides. As the majority of the sperm is blocked in the J3 layer, we may deduce that these oligosaccharides are used primarily for protection. They also select the sperm that is eventually allowed to fertilize the egg. The J1 and J2 layers are important for fertilization and blockage of polyspermy. The sulfated oligosaccharides are found only in these layers so that we may assume that they play the central role in both of these processes. The sulfated oligosaccharides may be the ligand for the cortical granule lectin that produces the block to polyspermy [14,15].

The combination of accurate mass and HPLC retention time is sufficient to identify oligosaccharides of known structures. Tandem MS, particularly CID, is necessary for confirming the identity and determining new unknown structures. These methods are general and will find uses in monitoring oligosaccharide diversity or changes in glycosylation in different samples and particularly in samples from different tissues. This method could find wide application in areas as diverse as cancer and infection.

Acknowledgments

The authors thank Dr. LeAnn Lindsay for helping in the collection of eggs. Funding provided by the National Institute of Health is greatly acknowledged.

References

[1] C. Katagiri, Fertilization of dejellied toad eggs in various experimental conditions, Embryologia 9 (1966) 159–163.
[2] J.L. Hedrick, T. Nishihara, Structure and function of the extracellular matrix of anuran eggs, J. Electron. Microsc. Tech. 17 (1991) 319–335.
[3] C. Katagiri, Role of oviducal secretiona in mediating gamete fusion in anuran amphibians, Zool. Sci. 4 (1987) 1–14.
[4] D.P. Wolf, J.L. Hedrick, A molecular approach to fertilization III: development of bioassay for sperm capacitation, Dev. Biol. 25 (1971) 360–376.
[5] S.B. Freeman, A study of the jelly envelopes surrounding the egg of the amphibian *Xenopus laevis*, Biol. Bull. 135 (1968) 501–513.
[6] E.D. Schmell, B.J. Gulyas, J.L. Hedrick, Egg changes during fertilization and the molecular mechanism of the block to polyspermy, in: J.F. Hartman (Ed.), Mechanism and Control of Animal Fertilization, 1983, pp. 365–413.
[7] J.S. Raisman, M.O. Cabada, Acrosomic reaction and proteolytic activity in the spermatozoa of an anuran amphibian, *Leptodactylus chaquensis*, Dev. Growth Differ. 19 (1977) 227–232.
[8] P. Jego, J. Joly, C. Boisseau, Amphibian jelly envelopes, proteins secreted by the oviduct and surrounding the eggs: their role in fertilization, Reprod. Nutr. Dev. 20 (1980) 557–567.
[9] Y. Shimoda, K. Kitajima, S. Inoue, Y. Inoue, Isolation, structural determination and calcium-binding properties of the major glycoprotein present in *Bufo japonicus* egg jelly, Eur. J. Biochem. 223 (1994) 223–331.
[10] J.R. Shaver, S.H. Barch, C.C. Umpierre, Interspecific relationships of oviduct materials as related fertilization in amphibian, J. Embryol. Exp. Morphol. 24 (1970) 209–225.
[11] K. Ishihara, J. Hosono, H. Kanatani, C. Katagiri, Toad egg-jelly as a source of divalent cations essential for fertilization, Dev. Biol. 105 (1984) 435–442.
[12] D. Reinhart, J. Ridgway, D.E. Chandler, *Xenopus laevis* fertilization: analysis of sperm mobility in egg jelly using video light microscopy, Zygote 6 (1998) 173–182.
[13] R.D. Gary, D.P. Wolf, J.L. Hedrick, Formation and structure of the fertilization envelope in *Xenopus laevis*, Dev. Biol. 36 (1974) 44–61.

[14] R.E Wyrick., T. Nishihara, J.L. Hedrick, Agglutination of jelly coat and cortical granule components and the block of polyspermy in the amphibian *Xenopus laevis*, Proc. Natl. Acad. Sci. USA 71 (1974) 2067–2071.
[15] L.C. Greve, J.L. Hedrick, An immunocytochemical localization of the cortical granule lectin in fertilized and unfertilized eggs of *Xenopus laevis*, Gamete Res. 1 (1978) 13–18.
[16] E.C. Yurewicz, G. Oliphant, J.L. Hedrick, The macromolecular composition of *Xenopus laevis* egg jelly coat, Biochemistry 14 (1975) 3101–3107.
[17] S. Koyato, S.K. Wimalasir, M. Hoshi, Structure of the main saccharide chain in the acrosome reaction-inducing substance of the startich, *Asterial amurensis*,, J. Biol. Chem. 272 (1997) 10372–10376.
[18] K. Tseng, Y. Xie, J. Seely, J.L. Hedrick, C.B. Lebrilla, Profiling with structural elucidation of the neutral and anionic O-linked oligosaccharides in the egg jelly coat of *Xenopus laevis* by Fourier transform mass spectrometry, Glycoconj. J. 18 (2001) 309–320.
[19] B.S. Bonnell, D.E. Chandler, Egg jelly layers of *Xenopus laevis* are unique in ultrastructure and sugar distribution, Mol. Reprod. Dev. 44 (1996) 212–220.
[20] B.S. Bonnell, D. Reinhart, D.E. Chandler, *Xenopus laevis* egg jelly coats consist of small diffusible proteins bound to a complex system of structurally stable networks composed of high-molecular-weight glycoconjugates, Dev. Biol. 174 (1) (1996) 32–42.
[21] K. Tseng, J.L. Hedrick, C.B. Lebrilla, The catalog-library approach for the rapid and sensitive structural elucidation of oligosaccharides, Anal. Chem. 71 (1999) 3747–3754.
[22] M.J. Davies, K.D. Smith, R.A. Carruthers, W. Chai, A.M. Lawson, E.F. Hounsell, Use of a porous graphitized carbon column for the high-performance liquid chromatography of oligosaccharides, alditols and glycopeptides with subsequent mass spectrometry analysis, J. Chromatogr. A 646 (1993) 317–326.
[23] K. Koizumi, High-performance liquid chromatographic separation of carbohydrates on graphitized carbon columns, J. Chromatogr. A 720 (1996) 119–126.
[24] J.Q. Fan, A.K. Kondo, K. Kato, Y.C. Lee, High-performance liquid chromatography of glycopeptides and oligosaccharides on graphitized carbon columns, Anal. Biochem. 219 (1994) 224–229.
[25] G. Strecker, J.-M. Wieruszeski, Y. Plancke, B. Boilly, Primary structure of 12 neutral oligosaccharide-alditols released from the jelly coats surrounding of the anuran *Xenopus laevis* by reductive beta-elimination, Glycobiology 5 (1995) 137–146.
[26] Y. Xie, K. Tseng, J.L. Hedrick, C.B. Lebrilla, Targeted use of exoglycosidase digestion for the structural elucidation of neutral O-linked oligosaccharides, J. Am. Soc. Mass Spectrom. 12 (2002) 877–884.
[27] Y. Guerardel, O. Kol, E. Maes, T. Lefebvru, B. Boilly, M. Davril, G. Strecker, *O*-Glycan variability of egg-jelly mucins from *Xenopus laevis*: characterization of four phenotypes that differ by the terminal glycosylation of their mucins, Biochem. J. 352 (2001) 449–463.
[28] J.L. Hedrick, A.J. Smith, E.C. Yurewicz, G. Oliphant, D.P. Wolf, Incorporation and fate of sulfate [^{35}S]-sulfate in the jelly coat of *Xenopus laevis* eggs, Biol. Reprod. 11 (5) (1974) 534–542.